Molecular Physics

An International Journal at the Interface Between Chemistry and Physics

ISSN: (Print) (Online) Journal homepage: https://www.tandfonline.com/loi/tmph20

Lamivudine adsorption on the novel borospherene as a promising drug delivery system: a DFT study on HIV therapy

Abduladheem Turki Jalil, Uday Abdul-Reda Hussein, Ali Abdulhussain Fadhil, Furqan S. Hashim, Ahmed Faisal, Zainab Hussein Adhab, Abbas F. Almulla & Hamed Soleymanabadi

To cite this article: Abduladheem Turki Jalil, Uday Abdul-Reda Hussein, Ali Abdulhussain Fadhil, Furqan S. Hashim, Ahmed Faisal, Zainab Hussein Adhab, Abbas F. Almulla & Hamed Soleymanabadi (18 Sep 2023): Lamivudine adsorption on the novel borospherene as a promising drug delivery system: a DFT study on HIV therapy, Molecular Physics, DOI: 10.1080/00268976.2023.2259503

To link to this article: https://doi.org/10.1080/00268976.2023.2259503

Published online: 18 Sep 2023.

MOLECULAR PHYSICS e2259503
https://doi.org/10.1080/00268976.2023.2259503

Taylor & Francis
Taylor & Francis Group

RESEARCH ARTICLE

Lamivudine adsorption on the novel borospherene as a promising drug delivery system: a DFT study on HIV therapy

Abduladheem Turki Jalil[a], Uday Abdul-Reda Hussein[b], Ali Abdulhussain Fadhil[c], Furqan S. Hashim[d], Ahmed Faisal[e], Zainab Hussein Adhab[f], Abbas F. Almulla[g] and Hamed Soleymanabadi[h]

[a]Medical Laboratories Techniques Department, Al-Mustaqbal University College, Hilla, Iraq; [b]College of Pharmacy, University of Al-Ameed, karbala, Iraq ; [c]College of Medical Technology, Medical Lab techniques, Al-Farahidi University, Iraq ; [d]Department of Medical Laboratories Technology, AL-Nisour University College, Baghdad, Iraq; [e]Department of Pharmacy, Al-Noor University College, Nineveh, Iraq; [f]Department of Pharmacy, Al-Zahrawi University College, Karbala, Iraq; [g]Medical Laboratory Technology Department, College of Medical Technology, The Islamic University, Najaf, Iraq; [h]Department of Chemistry, Central Tehran Branch, Islamic Azad University, Tehran, Iran

ABSTRACT

The present study investigates the utilisation of density functional theory (DFT) to examine unmodified and amino acid-functionalised C_4B_{32} borospherenes as potential carriers for drug transport. The recent and significant finding of borospherenes, which are composed of a cluster of four carbon atoms fused into a $B_{36}{}^{4-}$ structure (referred to as C_4B_{32}), has provided a valuable opportunity to explore the potential capabilities of unmodified and alanine-modified C_4B_{32} clusters as efficient vehicles for medicinal substances. The main objective of this study was to utilise Density Functional Theory (DFT) to examine the interaction between unmodified and alanine-linked borospherenes and the medicinal substance Lamivudine (LV). The investigation results revealed that the incorporation of amino acids had a pivotal role in facilitating the distribution of bio-drugs, leading to an improvement in the binding capacity of the C_4B_{32} cluster with the drug.

In this study, the dispersion-corrected density functional theory (DFT) approach proposed by Grimme examined long-range interactions. The calculations were performed utilising the B3LYP functional, implemented with the 6–31 + G(d) basis set in the GAMMES software. The electronic spectra of the drug@cluster complexes were analyzed using UV-Vis calculations, revealing a noticeable shift towards longer wavelengths, commonly called redshift. The results above highlight the significant potential of alanine-modified C_4B_{32} borospherenes in drug delivery applications.

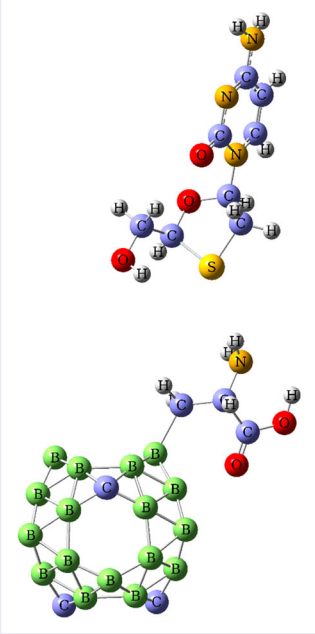

ARTICLE HISTORY
Received 25 August 2023
Accepted 11 September 2023

KEYWORDS
C_4B_{32}; modification; Lamivudine; borospherenes

CONTACT Hamed Soleymanabadi soleymanabadi.iau@gmail.com

1. Introduction

Chronic hepatitis B (HBV) and human immunodeficiency virus (HIV) continue to pose substantial difficulties in public health on a global scale. Hepatitis has a prevalence of over 300 million cases, whereas HIV affects a population of 33.2 million individuals [1, 2]. Lamivudine is classified as a nucleoside analog or reverse transcriptase inhibitor drug class member. From a therapeutic standpoint, this chemical can be classified as a synthetic nucleoside analog of cytidine. Upon being administered, it undergoes phosphorylation processes within the human body, resulting in the formation of metabolites that exhibit biological activity. The medicine in question has been granted approval for the treatment of Human Immunodeficiency Virus (HIV), the etiological agent responsible for Acquired Immune Deficiency Syndrome (AIDS) [3], as well as for both acute and chronic hepatitis B [4, 5].

Lamivudine (LV) is classified chemically as (2R,5S)−4-amino-1-(2-hydroxymethyl-1,3-oxathiolan-5-yl)-(1H). The field of pharmaceutical delivery is currently experiencing significant progress as it explores the utilisation of nanoparticle technology. This discipline aims to optimise pharmaceutical substances' pharmacological and therapeutic properties while minimising potential hazards using nanoscale drug delivery systems [6, 7].

The unique electrical and structural characteristics of boron, when compared to carbon in the periodic table, play a fundamental role in its exceptional adaptability as an element. Numerous investigations have been carried out to examine a wide range of structural arrangements, such as nanotubes, boron sheets, and cages [8–17]. Considerable academic attention has been devoted to the prominent attributes of pristine boron nanoclusters, including their elevated melting points, conductivity, and lightweight nature. The broad range of boron nanoclusters includes polyhedral boranes and their derivatives. The phenomenon of forming triangulated polyhedra interconnected through two-center or three-center connections has been documented in these nanoclusters. Considerable computational efforts have been devoted to exploring nanoclusters, commencing with identifying B_{80} nanoclusters [18–28]. Extensive and in-depth scholarly inquiry, incorporating both theoretical and empirical analyses, has revealed the existence of nanoclusters of varying sizes, such as B_{30} and B_{35-36} [29–35]. Academic researchers conducted thorough and rigorous investigations, employing a combination of theoretical analysis and experimental validation, to identify B_{39}, B_{40}, B_{41}^{+}, and B_{42}^{+} nanoclusters as borospherenes. The scholars above introduced 'borospherenes' in their previous work [36–38]. Previous research efforts have effectively found stable clusters, such as triangular B cages containing hexagonal gaps [39–47]. The extant literature on the B_{40} borospherene has thoroughly investigated its possible uses in several fields, including gas separation, sensing, and hydrogen storage [48, 49]. The endeavour to characterise and generate B_{36}^{4-} as a cluster with a cubic structure consisting exclusively of hexagonal forms and four extra electrons offered considerable difficulties. To tackle this issue, carbon was implemented as a replacement for boron, resulting in the successful stabilisation of the B_{36}^{4-} ion and the subsequent neutralisation of its negative charge. The invention above facilitated a systematic investigation and subsequent identification of the C_4B_{32} nanocluster [50, 51]. The chemical under investigation has been subject to a theoretical examination, which has revealed its significant stability and prospective applications in gas separation.

An in-depth analysis was conducted using density-functional theory (DFT) to examine the properties of C_4B_{32} and its potential use in drug delivery systems. The present study investigated the relationships between the C_4B_{32} nanocluster, alanine-functionalised C_4B_{32} clusters, and their binding interactions with LV. Furthermore, a comprehensive assessment was performed to evaluate the stability of the C_4B_{32} cluster functionalised with alanine, as well as its influence on the adsorption capacity of LV. Multiple metrics were calculated and analyzed, including adsorption energy, electrical properties, molecule electrostatic potential, ultraviolet–visible spectra, and density of states (DOS).

2. Computational details

In this study, the authors utilised density functional theory (DFT) calculations to investigate the energetic properties of a LV medication about unmodified C_4B_{32} nanoclusters and alanine-functionalised C_4B_{32} clusters (ala@ C_4B_{32}). In this study, the dispersion-corrected density functional theory (DFT) approach proposed by Grimme [52] examined long-range interactions. The calculations were performed utilising the B3LYP functional [53, 54], implemented with the 6-31 + G(d) basis set in the GAMMES software. The believability of this theoretical framework within the realm of boron-based nanoclusters has been established in prior research. Vibrational frequency calculations were performed to verify that the best geometry corresponds to local minima. The convergence criteria included a condition that the density variation should be smaller than 10×10^{-6} in absolute magnitude between consecutive iterations of the self-consistent field algorithm. Additionally, various default programme parameters for optimisation were taken into account.

The Basis Set Superposition Error (BSSE) was computed to correct the adsorption energy (E_{ads}) by considering the overlap of basis functions. The determination of the adsorption energy of the LV medication onto the nanoclusters was accomplished through the utilisation of the subsequent formula:

$$\text{Eads} = \text{E(LV/nanocluster)} - \text{E(nanocluster)} - \text{E(LV)} + \text{E}_{\text{BSSE}}$$

The equation is utilised to calculate the adsorption energy (Eads). The energy of a grain boundary (LV) in a nanocluster system, denoted as E_{ads}, can be expressed as the difference between the energy of the nanocluster with the LV (E (LV/nanocluster)), the energy of the nanocluster without the LV (E (nanocluster)), the energy of the LV (E (LV)), and the energy contribution from the basis set superposition error (E_{BSSE}).

The variable 'E_{ads}' is utilised to express the adsorption energy of a gas molecule on a nanocluster, which is defined as E(LV/nanocluster). The energy associated with a nanocluster, denoted as E(nanocluster), can be ascertained by subtracting the energy attributed to a grain boundary, represented as E(LV), from the energy associated with the bulk solid-state effect, denoted as E_{BSSE}.

In the present context, the symbol E(LV/nanocluster) represents the aggregate energy of the LV medication following its adsorption onto the nanocluster. The symbol E(nanocluster) denotes the aggregate energy of the nanocluster in its unconnected condition, while E(LV) reflects the collective energy of the LV drug in its unbound form. Exothermic adsorption is indicated by the presence of negative values for E_{ads}. The primary focus of the work was to investigate the electrical properties of the nanoclusters about the adsorption of LV. The achievement was attained through the computation of the energy gap (Eg), which denotes the disparity between the highest occupied molecular orbital (HOMO) and the lowest unoccupied molecular orbital (LUMO) levels. The charge transfers between the drug molecules and the nanoclusters was also evaluated by measuring natural bond orbitals [55].

3. Results and discussion

Figure 1 illustrates the structural characteristics of three entities: the unmodified C_4B_{32} cluster, the C_4B_{32} cluster functionalised with alanine (ala-C_4B_{32}), and the optimised LV molecule. The presence of amino acid-functionalised systems resulted in noticeable improvements in stability, as observed in the case of ala- C_4B_{32}. This compound consists of two separate isomeric forms, namely ala- C_4B_{32}-2 and ala- C_4B_{32}-1. The compound ala- C_4B_{32} −2 exhibits covalent bonding between the amino acid alanine and the boron atoms in the C_4B_{32} molecule. On the other hand, in the context of ala- C_4B_{32} −1, the amino acid alanine forms covalent connections with the carbon atoms present in the C_4B_{32} framework.

The tetrahedral structure of the C_4B_{32} cluster, as shown in Figure 1a, is characterised by four carbon atoms positioned at the vertices. The carbon atoms in this system are connected by C–C bonds ranging from 3.19–4.73 Å. There are two types of carbon atoms: C-1, located at the open edges surrounding a single void in C_4B_{32}, and C-2, positioned at the open edges adjacent to a pair of voids within the cluster. The average bond lengths between carbon–boron (C-B) and boron-boron (B-B) within the unaltered C_4B_{32} cluster are recorded correspondingly as 1.51 and 1.64 Å.

Based on the calculations conducted, it has been determined that alanine forms bonding connections with carbon and boron atoms inside the C_4B_{32} cluster. This interaction leads to forming two stable configurations, ala- C_4B_{32}-1 and ala- C_4B_{32}-2. Furthermore, the introduction of the alanine amino acid leads to the elongation of the B-C and B-B bonds next to the functionalised areas in the isomers ala- C_4B_{32}-1 and ala- C_4B_{32}-2. The modification causes an enlargement of the B-B and C-B bonds neighbouring the bonded areas, leading to augmentation from the initial C_4B_{32} structure's bond lengths of 1.64 and 1.51 Å to 1.91 Å in the ala- C_4B_{32}-2 isomer and 1.68 Å in the ala- C_4B_{32}-1 isomer, respectively.

The molecular arrangement in ala- C_4B_{32}-1 involved enhanced intermolecular interactions between the carbon atoms of alanine and the carbon atom of C_4B_{32}. This differs from ala- C_4B_{32}-2, where the bonding occurred between the cluster and the carbon atom of the amino acid. The reduced interatomic distance between carbon–carbon (C–C) atoms promotes efficient charge transfer, increasing the alanine-functionalised cluster's overall stability. Figure 2 presents electrostatic potential maps of the clusters, with regions exhibiting increased charge density represented by red, while areas with decreased charge density are portrayed in blue. An isosurface value of 0.0004 atomic units was employed to investigate the electrostatic potential.

The examination of the distribution of electrostatic potential reveals that the boron atoms near the C-1 atoms inside the C_4B_{32} molecule (as denoted by the blue patches) are strategically situated to attract nucleophilic agents. Likewise, the charge density exhibits a greater concentration within the vacant sections of C_4B_{32}, as indicated by red patches. As a result, these empty spaces become appealing locations for electrophilic reagents. The alanine-functionalised isomers, ala- C_4B_{32}-1 and

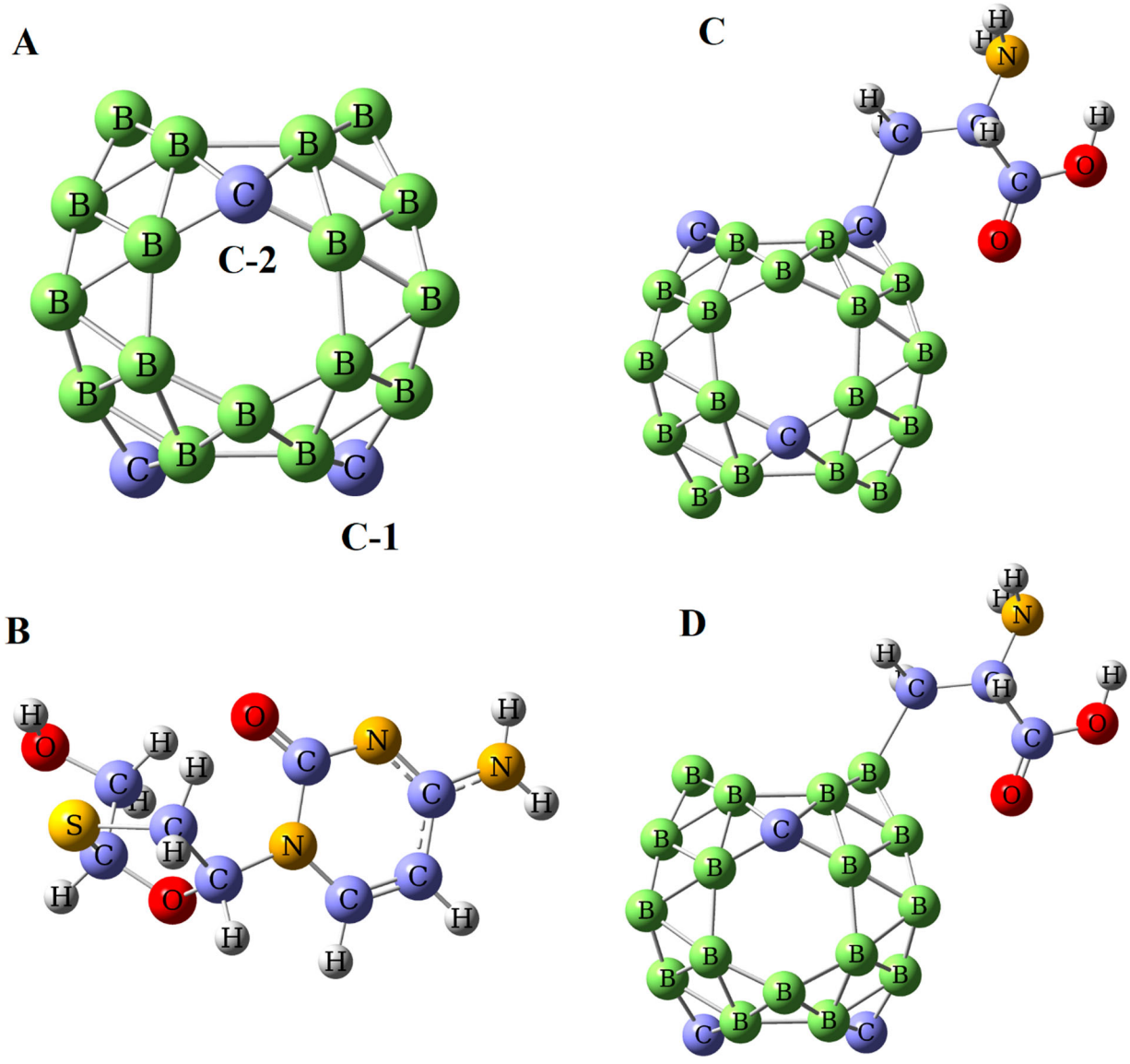

Figure 1. Optimum structure of pristine C_4B_{32} (A), LV drug (B), ala-C_4B_{32}-1 (C) and ala-C_4B_{32}-2(D).

ala- C_4B_{32}-2, exhibit distinct preferences for nucleophilic and electrophilic agents. Specifically, alanine sites are favoured for nucleophilic interactions, whereas pure voids are favoured for electrophilic interactions.

Figure 2 presents an aerial perspective of the frontier molecular orbitals (FMOs) of unmodified C_4B_{32} clusters and their alanine-functionalised counterparts. It is worth mentioning that the energy levels of the highest occupied molecular orbital (HOMO) and lowest unoccupied molecular orbital (LUMO) in the virgin C_4B_{32} exhibit a homogeneous distribution over the surface of the cluster. In contrast, the energy levels of the highest occupied molecular orbital (HOMO) and lowest unoccupied molecular orbital (LUMO) in the clusters functionalised with alanine are situated at the C_4B_{32} cage, as opposed to being centred on the alanine moiety.

Examining natural bond orbitals indicates that the boron atom in the unaltered C_4B_{32} cluster carries a positive charge of +0.297 e. In contrast, the C-1 and C-2 atoms bear negative charges of −0.760 e and −0.801 e, respectively. The atomic charges on the B, C-1, and C-2 atoms of the alanine-functionalised clusters, specifically ala- C_4B_{32}-1 and ala- C_4B_{32}-2, were determined to be +0.311, −0.823, and −0.920 e, respectively, through calculations. The observation above indicates a significant charge transfer from boron to carbon atoms within the nanoclusters.

The energy gap (Eg) values for C_4B_{32}, ala- C_4B_{32} −1, and ala- C_4B_{32} −2 are found to be 3.48, 2.05, and 2.30 eV, respectively. The Eg above values are consistent with the findings reported in the extant literature about the C_4B_{32} nanocluster. The electronic characteristics of

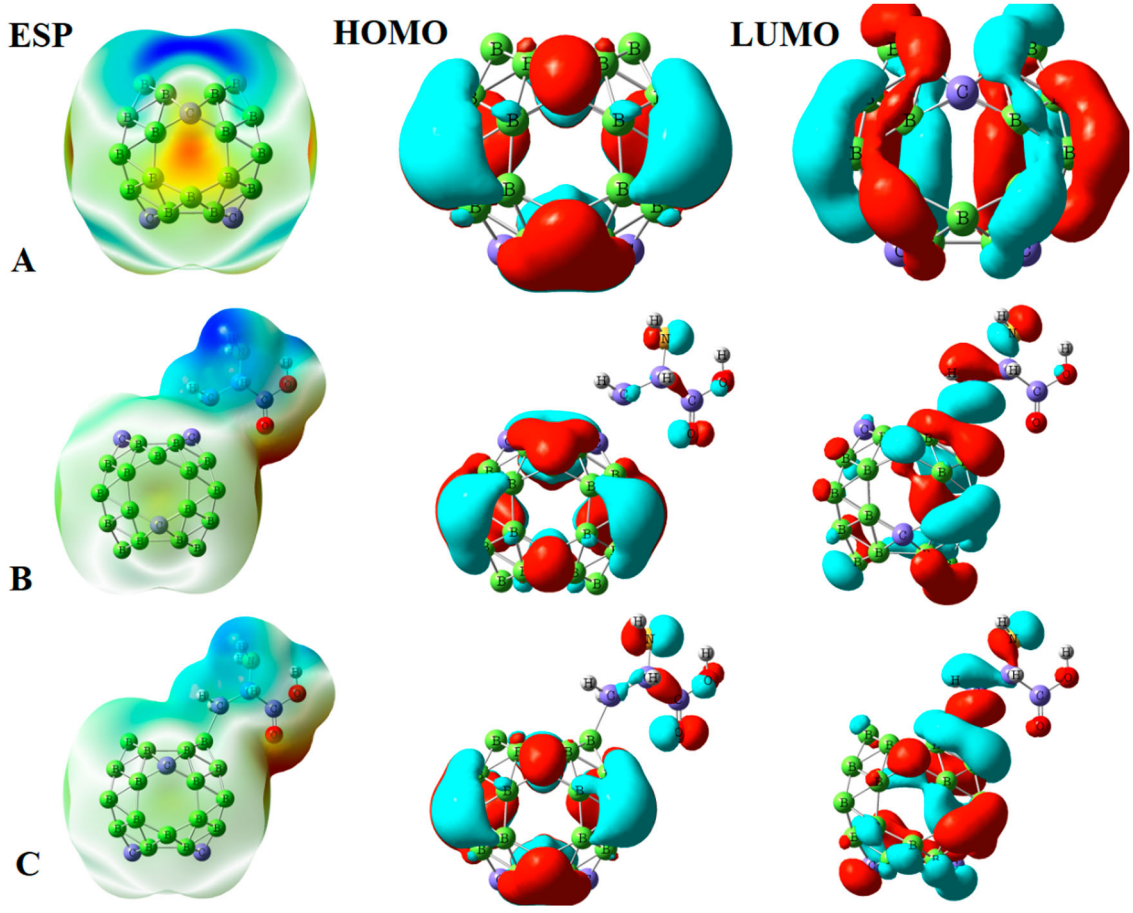

Figure 2. Electrostatic potential and frontier molecular orbital analyses of the pristine C_4B_{32} (A), ala-C_4B_{32}-1 (B), and ala-C_4B_{32}-2 (C) systems.

the borospherene cluster are confirmed to be affected by alanine functionalization and the presence of carbon atoms, as demonstrated by the density of states (DOS) measurements depicted in Figure 3.

The analysis of Figure 3a indicates that the partial density of states (DOS) centred at the 4C location of C_4B_{32} exhibits hybridisation with the B_{32} state in the regions corresponding to the highest occupied molecular orbital (HOMO) and lowest unoccupied molecular orbital (LUMO). Moreover, large modifications in the density of states (DOS) on both sides of the Fermi levels occur due to significant interactions between C_4B_{32} and the alanine amino acid. The isomers ala- C_4B_{32}-1 and ala-C_4B_{32}-2 demonstrate significant alterations in the energy levels of both the conduction and valence bands. Consequently, there is a clear decrease in the cluster's energy gap (Eg).

The analysis of Figures 3b and c reveals that the incorporation of alanine results in a LUMO (lowest unoccupied molecular orbital) with reduced energy, hence causing a decline in the energy gap (Eg). Significantly, the energy gaps (Eg) observed in the ala- C_4B_{32}-2 and ala- C_4B_{32}-1 isomers are notably less than that of the C_4B_{32} isomer, with reductions of 33% and 41%, respectively. The ala- C_4B_{32}-2 isomer exhibits an energy gap (Eg) of 2.33 electron volts (eV), whereas the ala- C_4B_{32}-1 isomer demonstrates an energy gap of 2.07 eV.

3.1. Adsorption of LV on alanine-functionalised and pristine C_4B_{32} borospherenes

A thorough investigation was undertaken to examine various geometries for the adsorption of LV onto unmodified and alanine-functionalised C_4B_{32} clusters. The optimised structures of several complexes, specifically LV@ C_4B_{32}, LV@ala-C_4B_{32}-1, and LV@ala-C_4B_{32}-2, are depicted in Figure 4. These structures were obtained by employing different initial arrangements. The study utilised a rigorous and unrestricted geometric optimisation approach to determine the maximum stability of LV@ C_4B_{32} systems. The results indicated that the most stable configurations were characterised by the adsorption of LV via nitrogen atoms, facilitating interactions with both the B and C atoms within the C_4B_{32} cluster.

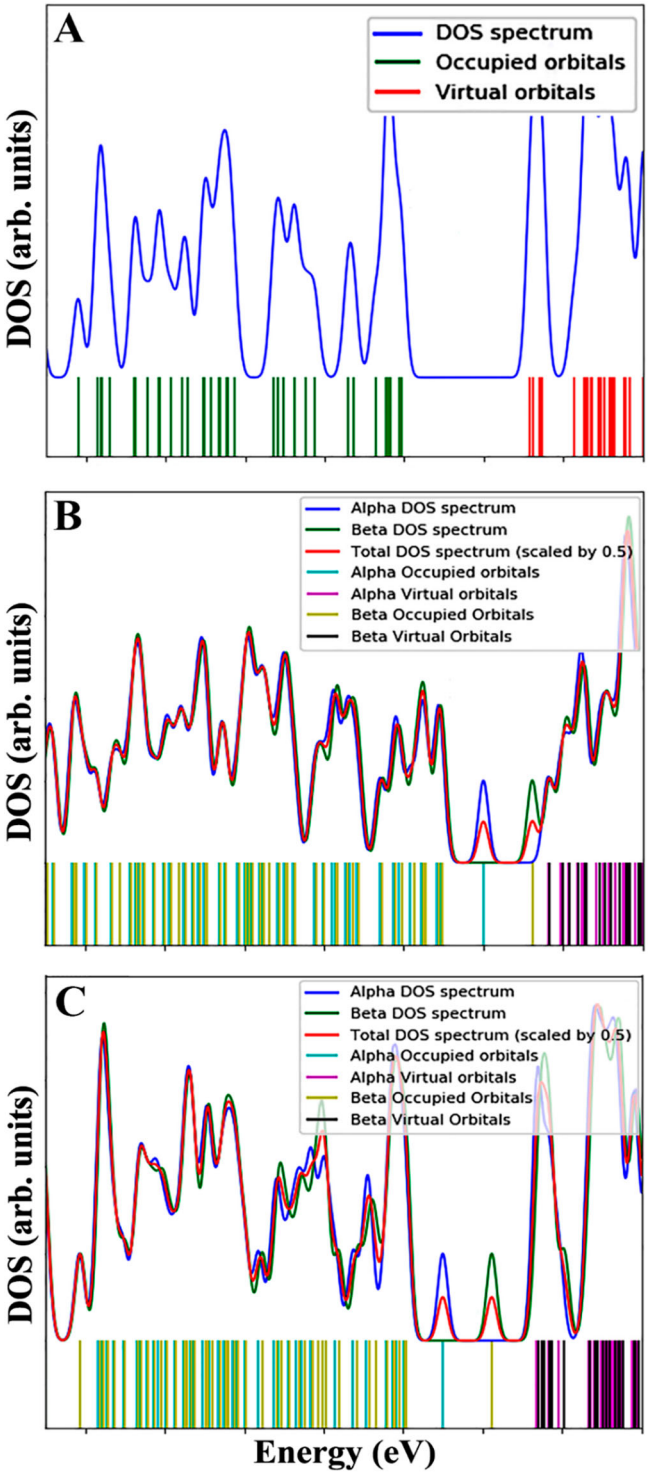

Figure 3. DOS plots for the pristine C_4B_{32} (A), ala-C_4B_{32}-1 (B), and ala-C_4B_{32}-2 (C) clusters.

Additionally, Figure 4 depicts the most stable configurations for the adsorption of LV on the amino acid chains and cages of ala- C_4B_{32}-1 and ala- C_4B_{32}-2 isomers. As illustrated in Figure 4a, the adsorption of LV occurs on the carbon atom of the unaltered C_4B_{32} structure. Similarly, the 4B species is adsorbed onto the boron atom inside the unaltered C_4B_{32} structure. Furthermore, it has been discovered that 4C exhibits adsorption onto an amino acid chain known as ala-C_4B_{32}-1, whereas 4D is adsorbed onto the carbon atom of ala-C_4B_{32}-1. Additionally, the compound 4E exhibits adsorption onto an amino acid chain known as ala-C_4B_{32}-2, while 4F is adsorbed onto the boron atom of the same ala- C_4B_{32}-2 molecule.

The observation of drug binding to the B atom of ala- C_4B_{32} was evident in both the LV@ala- C_4B_{32}-2 and LV@ala-C_4B_{32}-1 complexes. The findings given in Table 1 provide significant insights into E_{ads} (adsorption energy) and interaction distances. Configurations B, D, and F demonstrated strong interactions characterised by interaction distances of around 1.40 Å. In contrast, it can be observed that configurations A, C, and E exhibit somewhat larger contact distances of 1.65, 1.82, and 1.74 Å, respectively, suggesting the presence of physisorption.

Moreover, the significantly increased E_{ads} values reported in configurations B, D, and F provide strong evidence for the chemisorption phenomenon of LV molecules onto the B atom of the unmodified alanine-functionalised nanoclusters. It is worth noting that the adsorption onto the B atoms of the clusters exhibited greater favorability than other systems. Furthermore, it is crucial to emphasise that the adsorption stability of graphene-based (LV) materials onto the cage structure of ala- C_4B_{32} isomers exhibited a notable superiority above LV's adsorption onto isolated alanine molecules. The observed higher E_{ads} values in configurations D and F can be ascribed to the reduced intermolecular distances between the nitrogen atoms of the LV drug and the boron atoms of the nanoclusters in these complexes, in contrast to the remaining configurations.

The results of the calculations emphasised the significant impact of alanine functionalization on enhancing the adsorption of the LV drug onto the C_4B_{32} nanocluster. The functionalization technique significantly improved the transportation of the drug for LV and greatly increased its interactions with the C_4B_{32} cluster. Furthermore, the study emphasised that the ala- C_4B_{32} isomers displayed more advantageous locations for the adsorption of LV.

The C_4B_{32} @cluster systems that exhibited the greatest positive charge on the B atoms and a more pronounced distribution of the LUMO level on the B atom had the highest E_{ads} values. These specific compounds were expected to embody the most favourable locations for nucleophilic agents to interact with, augmenting adsorption.

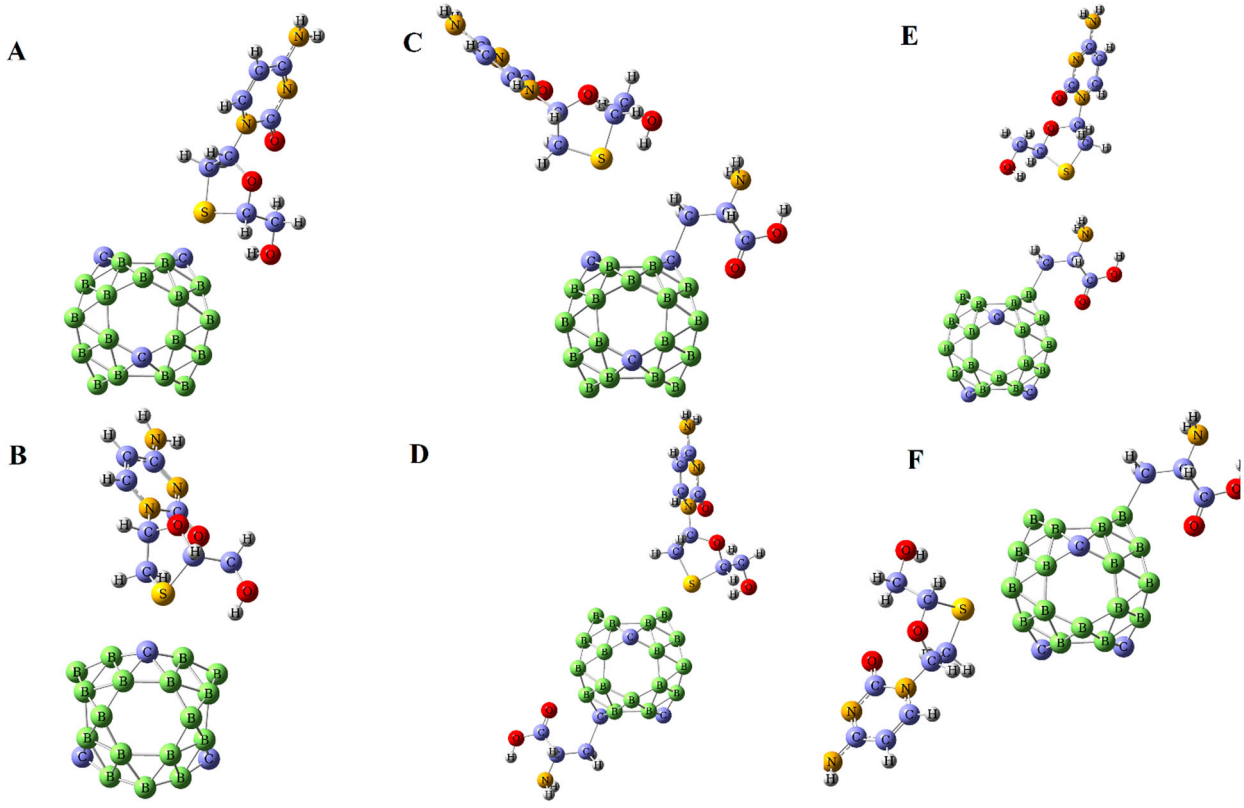

Figure 4. The most stable configurations of LV@C_4B_{32} ((A) and (B) panels), LV@ala-C_4B_{32}-1((C)and (D) panels), and LV@ala-C_4B_{32}-2 ((E) and (F) panels) systems.

Table 1. The calculated Eads and interaction distances in the LV@nanocluster complexes for the models (A) – (F) in Figure 4.

Configuration	Involved atoms	r(Å)	E_{ads} (kcal mol^{-1}) +BSSE
(A)	N (drug) – C (C_4B_{32})	1.65	−6.55
(B)	N (drug) – B (C_4B_{32})	1.42	−14.14
(C)	N (drug) – H (alanine)	1.82	−10.88
(D)	N (drug) – B (C_4B_{32})	1.41	−17.54
(E)	N(drug) – H (alanine)	1.74	−9.89
(F)	N (drug) – B (C_4B_{32})	1.40	−18.21

3.2. Solvent effect

The inquiry encompassed an examination of the adsorption of LV on clusters present in an aqueous phase. The objective of this study is to evaluate the influence of the solvent. Specifically, water possesses a dielectric constant denoted as $\epsilon = 78.4$. The polarised continuum model, alternatively referred to as the integral-equation formalism, was implemented to accomplish this objective.

In the solvent phase, configurations A through F exhibited much greater negative E_{ads} values, with measurements of −8.44, −19.22, −10.11, −22.78, −12.76, and −24.21 kcal/mol, respectively. The implications of these observations suggest that borospherenes can increase their solubility, hence causing changes in their interactions with the LV drug in a solvent environment.

3.3. The ultraviolet–visible (UV-Vis) spectrum

A TD-B3LYP-D3/6-31 + G (d) calculation was performed to ascertain the crucial excited states pertinent to the interaction between LV and the cluster. The results of the UV-Vis spectroscopic investigation on the unmodified cluster, the C_4B_{32} cluster functionalised with alanine, and the complexes formed with LV@cluster are displayed in Table 2.

Significantly, the spectra of the unaltered C_4B_{32}, ala-C_4B_{32}-2, and ala- C_4B_{32}-1 demonstrated their maximum absorption wavelengths (λ) at 428, 468, and 462 nm. The values above represent oscillator strengths, specifically 0.0722, 0.0848, and 0.0499, in the given order.

Table 2. Calculated oscillator strengths (*f*), maximum adsorption wavelength (λ), and dominant transition contribution for the pure clusters as well as drug/cluster complexes.

System	λ (nm)	*f*	Major contribution
C_4B_{32}	428	0.0722	HOMO→LUMO (55%)
(A)	451	0.0678	HOMO→LUMO (54%)
(B)	483	0.0143	HOMO→LUMO (62%)
ala – C_4B_{32}-1	462	0.0499	HOMO→LUMO (62%)
(C)	483	0.0661	HOMO→LUMO (65%)
(D)	521	0.0669	HOMO→LUMO (73%)
ala – C_4B_{32}-2	468	0.0848	HOMO→LUMO (66%)
(E)	504	0.0865	HOMO→LUMO (61%)
(F)	553	0.0945	HOMO→LUMO (73%)

The detected peaks at λ mostly corresponded to transitions between the highest occupied molecular orbital (HOMO) and the lowest unoccupied molecular orbital (LUMO). The electronic spectrum of the LV/cluster was observed to undergo a redshift towards longer wavelengths using time-dependent density functional theory (DFT) simulations. The configuration denoted as F exhibited a significant blue shift of 85 nm about the initial ala- C_4B_{32}-2 structure.

4. Conclusion

The main aim of this study was to examine the adsorption characteristics of the LV medicine on amino acid-functionalised and pristine C_4B_{32} borospherenes. The adsorption energies were analyzed upon incorporation of alanine, revealing a significant improvement in the adsorption capabilities of the borospherene. Regarding the strength of bonding within the complexes, it was observed that LV@ala- C_4B_{32} displayed the greatest E_{ads} value and exhibited a notable positive charge on its B atoms. The UV-Vis calculations demonstrated a redshift in the electronic spectra of the drug@cluster complexes, indicating a displacement towards longer wavelengths. The results presented provide solid empirical support for the considerable capacity of alanine-modified C_4B_{32} borospherenes to enhance the efficacy of medication transportation. The outcomes of this work highlight the practical utility of carriers such as alanine-functionalised C_4B_{32} borospherene in the context of drug delivery applications.

Disclosure statement

No potential conflict of interest was reported by the author(s).

References

[1] J.E. Maynard, Vaccine. **8**, S18 (1990). doi:10.1016/0264-410X(90)90209-5

[2] H.L. Wong, N. Chattopadhyay, X.Y. Wu and R. Bendayan, Adv. Drug Delivery Rev. **62**, 503 (2010). doi:10.1016/j.addr.2009.11.020

[3] N.L. Siegfried, P.J. Van Deventer, F.A. Mohomed and G.W. Rutherford, Cochrane Database Syst. Rev. **12**, CD004535 (2006).

[4] F. Hu, X. Xi and Y. Zhang, Technol. Forecast. Soc. Change. **169**, 120797 (2021). doi:10.1016/j.techfore.2021.120797

[5] G. Cui, K. Zhao, K. You, Z. Gao, T. Kakuchi, B. Feng and Q. Duan, Sci. Technol. Adv. Mater. **21** (1), 1–10 (2020). doi:10.1080/14686996.2019.1700394

[6] G. Cui, Y. Bai, W. Li, Z. Gao, S. Chen, N. Qiu, T. Satoh, T. Kakuchi and Q. Duan, Materials Science and Engineering: C. **78**, 603–608 (2017). doi:10.1016/j.msec.2017.03.059

[7] A.A. Bhirde, V. Patel, J. Gavard, G.F. Zhang and A.A. Sousa, ACS Nano. **3**, 307 (2009). doi:10.1021/nn800551s

[8] Y. Liu, T. Xu, Y. Liu, Y. Gao and C. Di, J. Mater. Res. Technol. **9** (4), 8283–8288 (2020). doi:10.1016/j.jmrt.2020.05.083

[9] L. Saedi, H. Soleymanabadi and A. Panahyab, Physica E. **99**, 106–111 (2018). doi:10.1016/j.physe.2018.01.027

[10] L. Saedi, S. Jameh-Bozorghi, M. Maskanati and H. Soleymanabadi, Inorg. Chem. Commun. **90**, 86–91 (2018). doi:10.1016/j.inoche.2018.02.011

[11] Z. Rostami and H. Soleymanabadi, J. Mol. Liq. **248**, 473–478 (2017). doi:10.1016/j.molliq.2017.09.126

[12] M. Noei, H. Soleymanabadi and A.A. Peyghan, Chem. Pap. **71** (5), 881–893 (2017). doi:10.1007/s11696-016-0015-5

[13] S. Jameh-Bozorghi and H. Soleymanabadi, Phys. Lett. A. **381** (6), 646–651 (2017). doi:10.1016/j.physleta.2016.11.039

[14] A. Rastgou, H. Soleymanabadi and A. Bodaghi, Microelectron. Eng. **169**, 9–15 (2017). doi:10.1016/j.mee.2016.11.012

[15] J. Hosseini, A. Bodaghi and H. Soleymanabadi, Russ. J. Phys. Chem. A. **91** (1), 116–123 (2017). doi:10.1134/S0036024417010095

[16] Z. Rostami and H. Soleymanabadi, J. Mol. Model. **22** (4), 70 (2016). doi:10.1007/s00894-016-2954-8

[17] V. Vahabi and H. Soleymanabadi, J. Mex. Chem. Soc. **60** (1), 34–39 (2016).

[18] S.F. Rastegar, H. Soleymanabadi and Z. Bagheri, J. Iran. Chem. Soc. **12** (6), 1099–1106 (2015). doi:10.1007/s13738-014-0570-z

[19] A.A. Peyghan, H. Soleymanabadi and Z. Bagheri, J. Iran. Chem. Soc. **12** (6), 1071–1076 (2015). doi:10.1007/s13738-014-0567-7

[20] A.A. Peyghan and H. Soleymanabadi, Curr. Sci. **108**, 1910–1914 (2015).

[21] S.F. Rastegar, A.A. Peyghan and H. Soleymanabadi, Physica E. **68**, 22–27 (2015). doi:10.1016/j.physe.2014.12.005

[22] N.L. Hadipour, A. Ahmadi Peyghan and H. Soleymanabadi, J. Phys. Chem. C. **119** (11), 6398–6404 (2015). doi:10.1021/jp513019z

[23] M. Nayebzadeh, H. Soleymanabadi and Z. Bagheri, Monatsh Chem.-Chem. Mon. **145** (11), 1745–1752 (2014). doi:10.1007/s00706-014-1239-0

[24] H. Soleymanabadi, Comput. Theor. Chem, 114302 (2023).

[25] M. Nayebzadeh, A.A. Peyghan and H. Soleymanabadi, Physica E. **62**, 48–54 (2014). doi:10.1016/j.physe.2014.04.016

[26] A.A. Peyghan, S.A. Aslanzadeh and H. Soleymanabadi, Monatsh Chem – Chem Mon. **145** (8), 1253–1257 (2014). doi:10.1007/s00706-014-1177-x

[27] H. Soleymanabadi and J. Kakemam, Physica E. **54**, 115–117 (2013). doi:10.1016/j.physe.2013.06.015

[28] H. Soleymanabadi and A.A. Peyghan, Comput. Mater. Sci. **79**, 182–186 (2013). doi:10.1016/j.commatsci.2013.06.027

[29] A.A. Peyghan, H. Soleymanabadi and M. Moradi, J. Phys. Chem. Solids. **74** (11), 1594–1598 (2013). doi:10.1016/j.jpcs.2013.05.030

[30] S.F. Rastegar, N.L. Hadipour, M.B. Tabar and H. Soleymanabadi, J. Mol. Model. **19** (9), 3733–3740 (2013). doi:10.1007/s00894-013-1898-5

[31] J. Beheshtian, H. Soleymanabadi, A.A. Peyghan and Z. Bagheri, Appl. Surf. Sci. **268**, 436–441 (2013). doi:10.1016/j.apsusc.2012.12.119
[32] J. Beheshtian, H. Soleymanabadi, M. Kamfiroozi and A. Ahmadi, J. Mol. Model. **18** (6), 2343–2348 (2012). doi:10.1007/s00894-011-1256-4
[33] Y. Mao and H. Soleymanabadi, J. Mol. Liq. **308**, 113009 (2020). doi:10.1016/j.molliq.2020.113009
[34] M. Li, Y. Wei, G. Zhang, F. Wang, M. Li and H. Soleymanabadi, Physica E. **118**, 113878 (2020). doi:10.1016/j.physe.2019.113878
[35] X. Wu, Z. Zhang and H. Soleymanabadi, Solid State Commun. **306**, 113770 (2020). doi:10.1016/j.ssc.2019.113770
[36] H. Goudarziafshar, M. Abdolmaleki, A.R. Moosavi-zare and H. Soleymanabadi, Physica E. **101**, 78–84 (2018). doi:10.1016/j.physe.2018.03.001
[37] R. Amirkhani, M.H. Omidi, R. Abdollahi and H. Soleymanabadi, J. Cluster Sci. **29** (4), 757–765 (2018). doi:10.1007/s10876-018-1398-y
[38] A.R. Moosavi-zare, M. Abdolmaleki, H. Goudarziafshar and H. Soleymanabadi, Inorg. Chem. Commun. **91**, 95–101 (2018). doi:10.1016/j.inoche.2018.03.017
[39] L. Saedi, M. Maskanati, M. Modheji and H. Soleymanabadi, J. Mol. Graphics Modell. **81**, 168–174 (2018). doi:10.1016/j.jmgm.2018.03.002
[40] B. Lin, H.L. Dong, C.M. Du, T.J. Hou, H.P. Lin and Y.Y. Li, Nanotechnology. **27**, 075501 (2016). doi:10.1088/0957-4484/27/7/075501
[41] H. Bai, M. Ma, J. Zuo, Q.-F. Zhang, B. Bai, H. Cao and W. Huanga, Phys. Chem. Chem. Phys. **21**, 15541–15550 (2019). doi:10.1039/C9CP02380A
[42] Z.A. Piazza, H.S. Hu, W.L. Li, Y.F. Zhao, J. Li and L.S. Wang, Nat. Commun. **5**, 3113 (2014). doi:10.1038/ncomms4113
[43] J. Zhang, Q. Shen, Y. Ma, L. Liu, W. Jia, L. Chen and J. Xie, Neurosci. Bull. **38**, 1267–1270 (2022). doi:10.1007/s12264-022-00899-6
[44] X. Song, Q. Li and J. Zhang, Biomed. Pharmacother. **162**, 114611 (2023). doi:10.1016/j.biopha.2023.114611
[45] J. Huang, Y. Jiang, W. Lin, R. Chen, J. Zhou, S. Guo, M. Zhao, Q. Xie, X. Chen, M. Zhao and Z. Zhao, ACS. Infect. Dis. **9** (6), 1221–1231 (2023). doi:10.1021/acsinfecdis.2c00601
[46] W. Lin, J. Huang, S. Guo, M. Zhao, X. Chen, Q. Shang, R. Zhang, G. Liao, J. Zheng and Y. Liao, J. Mater. Chem. B. **11** (20), 4523–4528 (2023). doi:10.1039/D3TB00747B
[47] J. Xia, Y. Li, C. He, C. Yong, L. Wang, H. Fu, X.L. He, Z.Y. Wang, D.F. Liu and Y.Y. Zhang, ACS. Infect. Dis. **9**, 1711–1729 (2023).
[48] T. Kato, T. Akasaka, K. Kobayashi, S. Nagase, K. Kikuchi, Y. Achiba, T. Suzuki and K. Yamamoto, J. Phys. Chem. Solids. **58**, 1779–1783 (1997). doi:10.1016/S0022-3697(97)00065-6
[49] Y. Tang, S. Liu, Y. Deng, Y. Zhang, L. Yin and W. Zheng, Biomed. Signal. Process. Control. **65** (2021). doi:10.1016/j.bspc.2020.102367
[50] S. Lu, B. Yang, Y. Xiao, S. Liu, M. Liu, L. Yin and W. Zheng, Biomed. Signal. Process. Control. **79**, 104204 (2023). doi:10.1016/j.bspc.2022.104204
[51] S. Lu, S. Liu, P. Hou, B. Yang, M. Liu, L. Yin and W. Zheng, Comput. Model. Eng. Sci. **136** (1), 363–379 (2023).
[52] S. Grimme, J. Comput. Chem. **27**, 1787 (2006). doi:10.1002/jcc.20495
[53] M. Ernzerhof and J.P. Perdew, J. Chem. Phys. **109**, 3313–3320 (1998). doi:10.1063/1.476928
[54] G.M. Barca, C. Bertoni, L. Carrington, D. Datta, N. De Silva, J.E. Deustua, D.G. Fedorov, J.R. Gour, A.O. Gunina, E. Guidez and T. Harville, J. Chem. Phys. **152** (15), 154102 (2020). doi:10.1063/5.0005188
[55] A. E. Reed, L. A. Curtiss, F. A. Weinhold, Chem. Rev. 88 (1998) 899-926. doi:10.1021/cr00088a005